

Complete phase diagram for three-band Hubbard model with orbital degeneracy lifted by crystal field splitting

Li Huang,^{1,2} Liang Du,¹ and Xi Dai¹

¹*Beijing National Laboratory for Condensed Matter Physics,
and Institute of Physics, Chinese Academy of Sciences, Beijing 100190, China*

²*National Key Laboratory for Surface Physics and Chemistry,
P.O. Box 718-35, Mianyang 621907, Sichuan, China*

(Dated: November 11, 2018)

Motivated by the unexplored complexity of the phase diagrams for multi-orbital Hubbard models, a three-band Hubbard model at integer fillings ($N = 4$) with orbital degeneracy lifted partially by crystal field splitting is analyzed systematically in this work. By using single site dynamical mean-field theory and rotationally invariant Gutzwiller approximation, we have computed the full phase diagram with Coulomb interaction strength U and crystal field splitting Δ . We find a large region in the phase diagram, where an orbital selective Mott phase will be stabilized by the positive crystal field lifting the orbital degeneracy. Further analysis indicates that the Hund's rule coupling is essential for the orbital selective Mott phase and the transition toward this phase is accompanied by a high-spin to low-spin transition. Such a model may be relevant for the recently discovered pnictides and ruthenates correlated materials.

PACS numbers: 71.10.Fd, 71.28.+d, 71.30.+h

I. INTRODUCTION

The Mott-Hubbard metal-insulator transition (MIT) has been a subject of great interest for decades.¹ Most of the attentions before this century have been focused on the one band case only, because most of the qualitative features of MIT have already been captured by single band Hubbard model, as shown by numerous studies using the single site dynamical mean-field theory (DMFT).² Whereas in realistic materials most of the Mott transitions involve more than one band and thus exhibit multi-orbital features.³ Multi-orbital extension of the Hubbard model allows more realistic description of MIT and other strongly correlated physics, which contains, in general, much richer phase diagrams, and exotic physical phenomena. For instance, the redistribution of electrons among different orbitals leads to new scenarios such as orbital ordering,⁴ high-spin to low-spin (HS-LS) transition⁵ or orbital selective Mott transition (OSMT)⁶ etc.

Mott transitions in multi-orbital models have been studied within the framework of DMFT for more than ten years.^{2,7} Previous studies show⁸ that simple increasing the band degeneracy only changes the critical interaction strength U_c , but will not change the fundamental features of Mott transition, where all the degenerate bands undergo Mott transition simultaneously under the increment of interaction strength. Recent studies of realistic materials have focused interest on the interplay between the MIT and orbital degeneracy.^{6,9-11} A very fundamental question raised in this field is, how the multi-orbital systems response to the breaking down of the orbital degeneracy. In such a system, it is possible that the Mott transitions in different orbitals happen separately, which is the so-called OSMT and has been suggested firstly by Anisimov *et al.*⁶ in the study of $\text{Ca}_{2-x}\text{Sr}_x\text{RuO}_4$.

After the concept of OSMT has been proposed, lots

of research interests have been attracted.¹²⁻²⁴ The early DMFT studies on this problem are focused on the two-band Hubbard model with half filling, which is the simplest system that may have OSMT when the bandwidths of the two bands are different. The DMFT calculations from different groups with exact diagonalization (ED)^{12,13} and Hirsch-Fye quantum Monte Carlo (HFQMC)¹⁴⁻¹⁸ as impurity solvers converge to two essential conclusions: (1) The OSMT in two-band Hubbard model is mainly induced by the bandwidth difference which breaks the degeneracy between the two bands and the crystal field splitting plays a minor role here. (2) The emergence of OSMT is very sensitive to the feature of the local interaction. It is very easy to occur OSMT when the local interaction is rotationally invariant, while very difficult to happen when the local interaction breaks the rotational invariance.

The OSMT in the three-band Hubbard model, which is more relevant to the realistic situation of $\text{Ca}_{2-x}\text{Sr}_x\text{RuO}_4$,^{6,22} is not a trivial generalization of the two-band model. In two-band systems, the OSMT can only happen in half filling case, while in three-band systems it can happen when the occupation numbers are 2, 3 or 4. When the total occupation number is 3, the three-band system is half filling and actually the situation is very similar with the two-band case. The most interesting case is when the occupation number is 2 or 4, which can be transformed between each other by particle-hole symmetry. Recently de' Medici *et al.*²³ proposed a new mechanism for OSMT, which happens in three-band systems with filling factor being 2 or 4. In this new scenario of OSMT, the driving force is not the difference of bandwidth but the crystal field splitting lifting the band degeneracy. And then Kita *et al.*²⁵ investigated how the orbital level splitting and Ising-type Hund's rule coupling affect the Mott transition in the case of two

electrons per site. Their results reveal that the critical interaction strength separating a metallic phase and two kinds of insulating phases shows a non-monotonic behavior as a function of the level splitting. They suggest that this behavior is characteristic for 1/3 filling, in comparison with the preceding results for different fillings and for two-band models. We note that the three-band system is very popular in transition metal compounds.^{1,3} Provided the Fermi energy falls into the t_{2g} bands, the tetragonal distortion will further split the t_{2g} bands into non-degenerate a_{1g} band and two-fold degenerate e'_g bands. When the occupation number is 4, the appropriate crystal field will redistribute the four electrons into a_{1g} band and e'_g bands as 1 and 3 respectively (i.e (3,1) configuration). Thus if we neglect the correlation between a_{1g} and e'_g sub-systems, the a_{1g} band becomes a one-band system at half filling and e'_g bands become a two-band system at quarter filling, which will lead to an orbital selective Mott phase (OSMP) at equal bandwidth because it is much easier to get Mott insulator in a_{1g} band. The mean-field phase diagram of this model determined by slave-spin method^{23,24} contains quite a large region for OSMP, in which the a_{1g} band has already become Mott insulator while the e'_g bands are still metallic.

The OSMT driven by the band degeneracy lifting is quite a robust phenomena determined by the interplay between crystal symmetry and correlation effects. In reference [23], the phase diagram of the three-band Hubbard model is mainly calculated by the slave-spin method, which is qualitatively correct but not accurate enough. In the present paper, we study systematically this t_{2g} Hubbard model with crystal field splitting by two more accurate methods: the DMFT method combined with state-of-the-art hybridization expansion continuous time quantum Monte Carlo (CTQMC) impurity solver²⁶⁻²⁹ and newly developed rotationally invariant Gutzwiller approximation (RIGA) method.³⁰⁻³³ The metal-insulator phase diagram, band specific quasiparticle weight Z_a and occupation number n_a are computed by the both methods with respect to crystal field splitting Δ and Coulomb interaction strength U . Based on these results, we mainly discuss three important aspects of OSMT in this system: (1) The crucial role of Hund's rule coupling; (2) The redistribution of four electrons among a_{1g} and e'_g bands; (3) The relationship between OSMT and HS-LS spin state crossover.

The rest of this paper is organized as follows: In Sec.II the three-band Hubbard model treated in this work is specified. In Sec.III A the main results of this paper, $U - \Delta$ phase diagrams for rotationally invariant interaction and $SU(N)$ density-density interaction are presented and compared with each other. In Sec.III B, the redistribution of electrons among different orbitals and its relationship with the OSMT are discussed in detail. And the accompanying HS-LS spin state crossovers are discussed in Sec.III C. Section IV serves as a conclusion.

II. MODEL

We consider the three-band Hubbard model defined by

$$H = - \sum_{i,j,a,\sigma} t_{ij} c_{ia\sigma}^\dagger c_{ja\sigma} + \sum_i H_{loc}^i, \quad (1)$$

where $c_{ia\sigma}^{(\dagger)}$ is an annihilation (creation) operator of an electron with spin σ ($=\uparrow, \downarrow$) and orbital a ($=1, 2, 3$) at the i th site, t_{ij} is the hopping integral between site i and site j . The local part of Hamiltonian H_{loc}^i can be defined as follows (for the sake of simplicity, the site index i has been ignored):

$$\begin{aligned} H_{loc} = & - \sum_{a,\sigma} (\mu - \Delta_a) n_{a,\sigma} + \sum_a U n_{a,\uparrow} n_{a,\downarrow} \\ & + \sum_{a>b,\sigma} [U' n_{a,\sigma} n_{b,-\sigma} + (U' - J) n_{a,\sigma} n_{b,\sigma}] \\ & - \sum_{a<b} J (d_{a,\downarrow}^\dagger d_{b,\uparrow}^\dagger d_{b,\downarrow} d_{a,\uparrow} + d_{b,\uparrow}^\dagger d_{b,\downarrow}^\dagger d_{a,\uparrow} d_{a,\downarrow} + h.c.). \end{aligned} \quad (2)$$

Here $n_{a,\sigma} = c_{a\sigma}^\dagger c_{a\sigma}$ is the number operator, μ is the chemical potential, and Δ_a is the energy level for orbital a . In the interaction terms, U (U') is the intra-orbital (inter-orbital) Coulomb interaction, and J is the Hund's rule coupling. The constrained condition $U = U' + 2J$ is imposed as usual, which is valid for atomic like local orbitals. The above interaction terms include both the spin-flip and pair-hopping terms, and thus are rotational invariant in the spin space. In order to elucidate the Mott MIT in the case of four electrons per site, the chemical potential μ is adjusted dynamically in the simulations to fix the electron filling per site as $N = 4$. In the present paper, we focus on the t_{2g} -like bands under the tetragonal crystal field, which are split into non-degenerate a_{1g} band and double degenerate e'_g bands. Therefore the on-site energy level is assumed to be $\Delta_1 \neq \Delta_2 = \Delta_3$ and their difference is defined as $\Delta = \Delta_1 - \Delta_2$.

This lattice model (see Eq.(1)) can be solved in the framework of single site DMFT^{2,7}, which neglects the momentum dependence of the self-energy and reduces the original lattice problem to the self-consistent solution of an effective impurity model. In this paper, a semicircular density of states with half bandwidth $D = 1$ is used, which corresponds to the infinite coordination Bethe lattice. All the orbitals have equal bandwidth and the energy unit is set to be D . To solve the effective impurity model, the hybridization expansion CTQMC impurity solver²⁶⁻²⁹ is adopted. This method allows us to access the strong interaction regime down to very low temperature. In our calculations, the system temperature is set to be $T = 0.01$ (corresponding to inverse temperature $\beta = 100$) unless otherwise stated. In each DMFT iterations, typically 4×10^8 QMC samplings have been performed to reach sufficient numerical accuracy.

In the present works, we also use the RIGA method³⁰⁻³³ to crosscheck the results obtained by

DMFT+CTQMC method. In contrast to the finite temperature DMFT+CTQMC calculations, only the zero temperature physical quantities can be obtained by using the RIGA method. Although the RIGA method can not access the dynamical properties of correlated systems, it provides a very fast and economic way to calculate the ground state properties, for examples, the total energy and occupation numbers. And it can be used as a good complementary method to the DMFT approach. As will be discussed in detail in the following sections, the phase diagrams and other physical properties obtained by both methods are in very good agreements. The implementation details about our RIGA method have been presented in reference [33].

III. RESULTS AND DISCUSSION

A. $U - \Delta$ phase diagram

To map out the metal-insulator phase diagram we have computed systematically the dependence of charge density, quasiparticle weight, and local magnetic moment as the function of crystal field splitting for various Coulomb interaction strengths. In this subsection, we will focus firstly on the $U - \Delta$ phase diagrams with both non-zero and zeroed Hund's rule coupling J . We will show in the following that the Hund's rule coupling J is extremely crucial for the appearance of OSMP in the three-band systems with four electrons.

When the spin-flip and pair-hopping interaction terms are taken into full considerations, the Hamiltonian for three-band Hubbard model is rotationally invariant in the spin space, and the phase diagram contains four different phases, which are metal, band insulator, OSMP and Mott insulator phases, respectively. The obtained $U - \Delta$ phase diagrams for $J = U/4$ case are illustrated in Fig.1. The upper panel is the results obtained by DMFT+CTQMC method, and the lower panel is obtained by RIGA method. From the above figure, we can easily see that the consistency between both two methods is quite excellent, except the phase boundary obtained by RIGA method is a bit higher, which is similar with the situations found in one and two-band models.^{32,33} Comparing with the similar phase diagrams obtained by slave-spin method in the literatures,^{23,24} there are two important differences. Firstly, the critical U_c for Mott transition at $\Delta = 0$ is much lower in the phase diagram obtained by DMFT+CTQMC method. Secondly, in the phase diagram obtained by both DMFT+CTQMC and RIGA methods, the phase boundary between the metal phase and band insulator phase depends on the interaction strength U monotonically, however in the phase diagram obtained by slave-spin method, it decreases firstly and then increases.²³ This difference is mainly due to the over simplified treatment of Hund's rule coupling terms in the slave-spin method.²⁴

The general shape of the phase diagram can be eas-

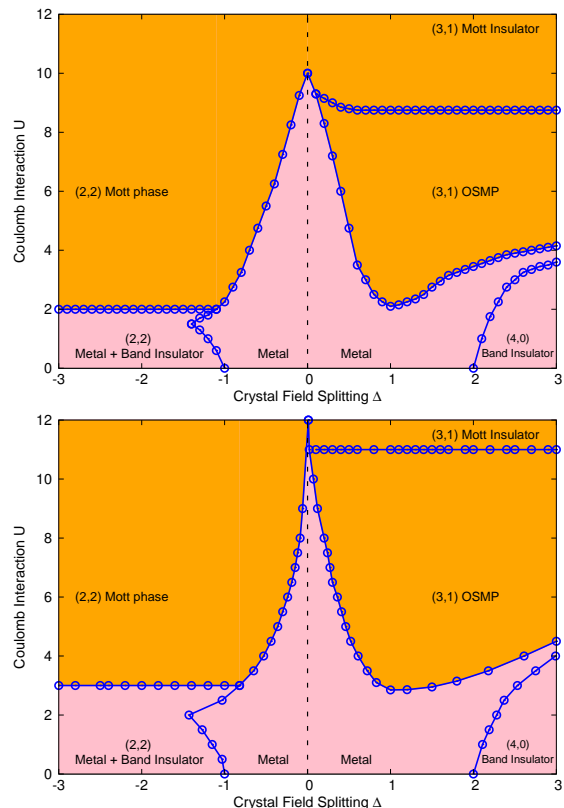


FIG. 1. (Color online) Calculated phase diagram of three-band Hubbard model with rotationally invariant interactions in the plane of Coulomb interaction U ($J = U/4$) and crystal field splitting Δ ($\Delta = \Delta_1 - \Delta_2$). Upper panel: Calculated by DMFT+CTQMC method at finite temperature $T = 0.01$. Lower panel: Calculated by RIGA method at zero temperature. In all the calculations, the chemical potential μ is adjusted dynamically to fulfill the total occupation number condition ($N = 4$). The label “(2,2) Metal + Band Insulator” means the two-fold degenerate bands (e'_g states) are metallic while the non-degenerate band (a_{1g} state) is insulating, and (2,2) means corresponding orbital occupancies. All the other labels have similar explanations. The pink zone means LS state and the orange zone means HS state respectively.

ily understood by considering two limiting cases: (1) For $\Delta = 0$, the model reduces to a fully degenerate three-band Hubbard model with total filling $N = 4$, which undergoes a Mott transition around $U = 10.0$; (2) For the uncorrelated limit ($U = 0$), when $\Delta > 0$, a simple transition from metal to band insulator can be observed at $\Delta = 2.0$ with the fully occupied e'_g bands and empty a_{1g} band. Another transition can also be seen on the negative side at $\Delta = -1.0$, after which the non-degenerate a_{1g} band is fully occupied band insulator and the double degenerate e'_g bands are metallic at half filling.

When both the Coulomb interaction U and crystal field Δ are non-zero, the phase diagram is quite complicated and very different for $\Delta > 0$ and $\Delta < 0$. Now let's make a further discussion about this phase diagram. If the crystal field splitting $\Delta > 0$, the isolate a_{1g} band is lifted

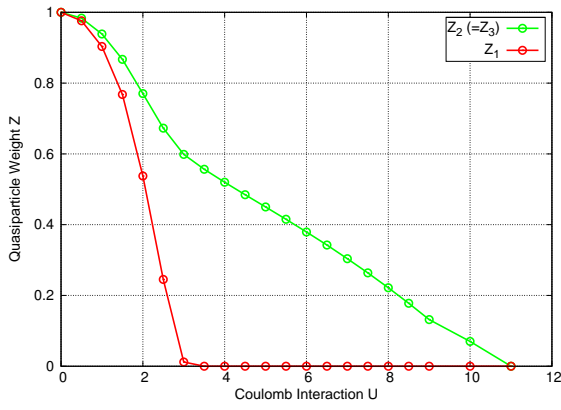


FIG. 2. (Color online) Quasiparticle weights Z_a as a function of Coulomb interaction U for selected crystal field splitting $\Delta = 1.0$. The calculations are done by the RIGA method at zero temperature.

up and the double degenerate e'_g bands are pushed down. This part of phase diagram can be divided vertically into two regions: (1) When $2.0 > \Delta > 0.0$, the system undergoes successive transitions from metal to Mott insulator through an OSMF as the Coulomb interaction strength increases; (2) When $\Delta > 2.0$, the system undergoes a different type of successive transitions from band insulator to Mott insulator through metal and OSMF phases in sequence. On the other hand, if the crystal field splitting $\Delta < 0$, i.e., the a_{1g} band is lower than the two-fold degenerate e'_g bands, this part of phase diagram can be divided into three different regions: (1) For $-1.0 < \Delta < 0.0$, with weak Coulomb interaction both bands have fractional filling and are metallic. As the increment of Coulomb interaction U , the system undergoes a transition from a fully metallic phase to an insulator phase, after which the occupation numbers for both a_{1g} and e'_g bands are two. Since the a_{1g} band has no degeneracy, it is completely occupied and becomes band insulator in this situation. While at the same time the e'_g bands with double degeneracy become Mott insulator with half filling. It is called (2,2) Mott insulator phase throughout this paper. (2) When $-1.4 < \Delta < -1.0$, with weak Coulomb interaction the a_{1g} band is already fully occupied and the double degenerate e'_g bands are half-filled and metallic. With the increment of Coulomb interaction U , the system first becomes fully metallic phase with fractional filling factors for all the bands, and then goes back to the original phase after a “reentrance” transition. Finally it becomes the (2,2) Mott insulator phase for $U > 2.0$. (3) When $\Delta < -1.4$, the a_{1g} band remains fully occupied regardless of the interaction strength and the system reduces to a two-band system with half filling, which undergoes a typical Mott MIT around $U = 2.0$ as determined by DMFT+CTQMC method.

We note that the effect of Coulomb interaction U have two important effects for multi-orbital systems. One is to reduce the quasiparticle weight, the other one is to

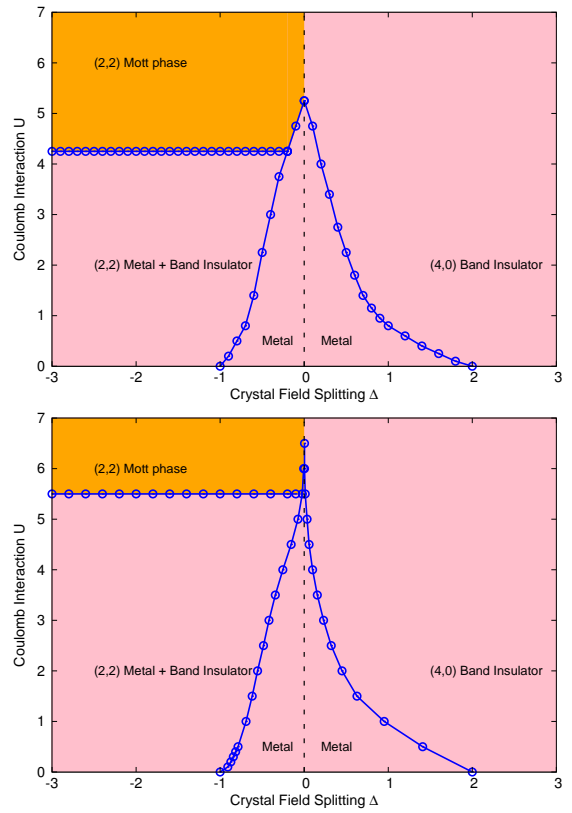


FIG. 3. (Color online) Calculated phase diagram of three-band Hubbard model with $SU(N)$ density-density interaction in the plane of Coulomb interaction U ($J = 0.0$) and crystal field splitting Δ ($\Delta = \Delta_1 - \Delta_2$). Upper panel: Calculated by DMFT+CTQMC method at finite temperature $T = 0.01$; Lower panel: Calculated by RIGA method at zero temperature. In the calculations, the chemical potential μ is adjusted dynamically to fulfill the total occupation number condition ($N = 4$). The label “(2,2) Metal + Band Insulator” means the two-fold degenerate bands (e'_g states) are metallic while the non-degenerate band (a_{1g} state) is insulating, and (2,2) means corresponding orbital occupancies. All the other labels have similar explanations. The pink zone means LS state and the orange zone means HS state respectively.

redistribute the electrons among different bands. The interplay between these two effects determines the main structure of the above phase diagram. Next we will focus on the first effect, and the second effect is less emphasized before and will be discussed in detail in the following subsections.

The band specific quasiparticle weights Z_a as a function of Coulomb interaction U are shown in Fig.2. The crystal field splitting is fixed to $\Delta = 1.0$. For simplicity, only the results obtained by RIGA method, which are consistent with those obtained by DMFT+CTQMC method, are displayed in this figure. It is apparent that the quasiparticle weights Z_a decrease monotonously from 1.0 to 0.0 when Coulomb interaction strength increases. As $U < 3.0$, the Z_a are large than 0.1, and both the e'_g and a_{1g} bands are metallic. As $U > 3.0$, Z_1 turns

to zero while $Z_2(=Z_3)$ is still finite. It means that the a_{1g} band undergoes a Mott MIT and turns into insulator at $U = 3.0$, and at the same time the e'_g bands keep metallic, which is the so-called (3,1) OSMP in the phase diagram. When Coulomb interaction strength continues to increase ($U > 11.0$ for the RIGA method and $U > 9.0$ for the DMFT+CTQMC method), the e'_g bands undergo another Mott MIT and the system becomes the (3,1) Mott insulator phase finally, then all Z_a will approach zero.

The Hund's rule coupling J has enormous influence on the metal-insulator phase diagram for multi-orbital Hubbard model.^{25,34} It is noted that if we neglect the spin-flip and pair-hopping terms, only keep the Ising-type Hund's rule coupling term $J_z (=J)$, we can obtain very similar phase diagram, albeit the phase boundary is shifted downwards slightly. It is apparent that the Ising-type Hund's rule coupling term J_z is the key requirement for OSMT and such a rich phase diagram. In order to reveal the underlying physics more clearly we also did calculations for the phase diagram of similar three-band Hubbard model without Hund's rule coupling terms ($J = 0$). Thus we can compare the $U - \Delta$ phase diagrams for the case with finite J (see Fig.1) and $SU(N)$ $J = 0$ case (see Fig.3). Obviously the latter is much simpler and has no OSMP in the whole phase diagram.

The calculated $U - \Delta$ phase diagram for $J = 0$ case is illustrated in Fig.3. The upper panel is the calculated results obtained by DMFT+CTQMC method, and the lower panel is obtained by RIGA method. These two methods give almost identical results again. Firstly we concentrate on the non-interaction case ($U = 0$). When the crystal field splitting is positive ($\Delta > 0$), an obvious transition can be seen at $\Delta = 2.0$ after which the system becomes band insulator. On the other hand, when crystal field splitting is negative ($\Delta < 0$), similar MIT can be found at $\Delta = -1.0$. When $\Delta > 0$, the phase diagram only consists of metal and band insulator phases. The lower left region is metallic, and the upper right region is band insulator phase. The OSMP is disappeared completely. When $\Delta < 0$, the phase diagram contains metal, band insulator, and Mott insulator phases, but the characteristic "tip" which can be clearly seen at $U \sim 1.0$ and $\Delta \sim -1.2$ in Fig.1 vanishes, and the phase boundary between metal plus band insulator and (2,2) Mott insulator is shifted upward significantly. Thus, it is concluded that the Hund's rule coupling terms J has played a key role on the phase diagram and finite J_z is the minimal requirement to drive an OSMT.

B. Redistribution of electrons

In this subsection, we will discuss the second important effect of Coulomb interaction U on multi-orbital systems with broken symmetry: the redistribution of electrons among different orbitals. In order to understand the intriguing physics contained in the $U - \Delta$ phase diagrams

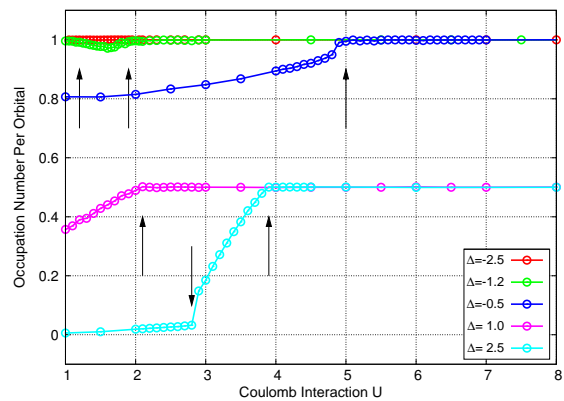


FIG. 4. (Color online) Orbital filling as a function of Coulomb interaction U for selected crystal field splitting Δ values (rotationally invariant interaction case). The results are calculated by DMFT+CTQMC method at finite temperature $T = 0.01$. In this figure, only the electron densities of non-degenerate band (a_{1g} band) are shown. The arrows correspond to phase transition points.

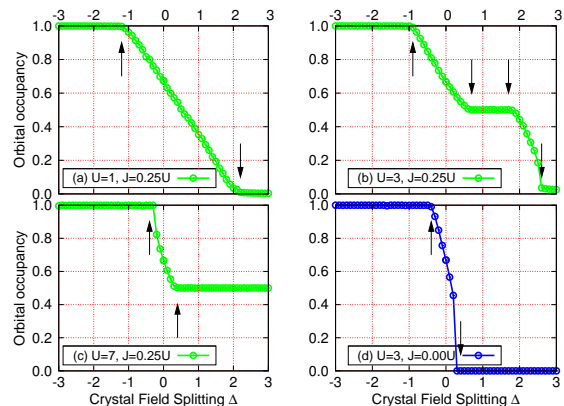


FIG. 5. (Color online) Orbital filling as a function of crystal field splitting Δ for selected Coulomb interaction U values. (a) $U = 1.0$; (b) $U = 3.0$; (c) $U = 7.0$; (d) $U = 3.0$. In (a)-(c), the interaction term is rotationally invariant with non-zero spin-flip and pair-hopping terms, whereas in (d) the interaction term is $SU(N)$ scheme with $J = 0$. All the calculations are done by DMFT+CTQMC method at finite temperature $T = 0.01$. In this figure, only the electron densities of non-degenerate a_{1g} band are shown. The arrows correspond to phase transition points.

more clearly, we further plot the occupation numbers of non-degenerate a_{1g} band as functions of Coulomb interaction U and crystal field splitting Δ in Fig.4~6, respectively.

In Fig.4, the evolution of the orbital occupancy with the Coulomb interaction strength is shown. The vertical arrows denote phase transition points. In this figure, only the orbital filling of the non-degenerate band (a_{1g} band) is plotted. For negative crystal field, a_{1g} band is much lower in energy, and the effect of Coulomb interaction depends on the value of the crystal field Δ in the following

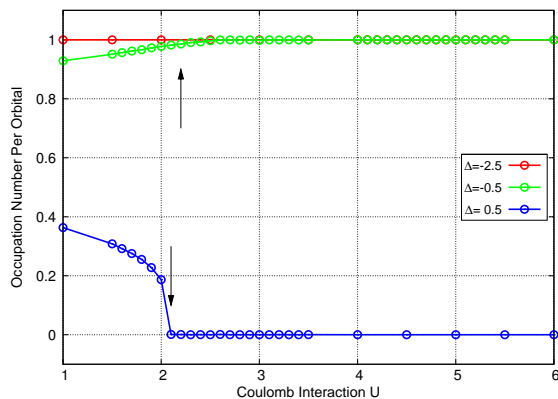


FIG. 6. (Color online) Orbital filling as a function of Coulomb interaction U for selected crystal field splitting values (SU(N) $J = 0$ case). All the calculations are done by DMFT+CTQMC method at finite temperature $T = 0.01$. In this figure, only the electron densities of non-degenerate a_{1g} band are shown. The arrows correspond to phase transition points.

way. For $0 > \Delta > -1.0$, the effect of correlation effect is to transfer electrons from e'_g bands to the a_{1g} band until it is fully occupied and becomes band insulator, as shown by the blue curve in Fig.4. For $-1.0 > \Delta > -1.4$, the a_{1g} band is already fully occupied in the non-interacting case and the effect of the correlation is non-monotonic. As the increment of the repulsive interaction U and Hund's rule coupling J , the occupation number of a_{1g} band first drops due to the Hund's rule coupling and then returns back to be fully occupied. We note that the interesting non-monotonic behavior of the occupation is the consequence of the interplay between Hund's rule coupling J , which favors even distribution of the electrons, and the Coulomb repulsive interaction U , which intends to increase the occupation difference between orbitals. Therefore, this behavior disappears when the Hund's rule coupling has been set to be zero, as shown in figure 6. While for $\Delta < -1.4$, the charge distribution will not be affected by the correlation effect and the occupation number of a_{1g} band keeps constant as the increment of U .

While the situation is very different for $\Delta > 0$, in this case the energy level of a_{1g} band is higher and the occupation number is less than 0.5 in the non-interacting case. As we can see from Fig.4, the increment of the interaction strength will pump the electrons from e'_g bands to a_{1g} band again until it reaches half filling and becomes Mott insulator. When the crystal field strength Δ is smaller than 2.0 all the bands are metallic, and the system becomes OSMP when the a_{1g} band reaches half filling. While for Δ is larger than 2.0, the system starts from a typical band insulator with fully occupied e'_g and empty a_{1g} bands. With the increment of Coulomb interaction, it first becomes metallic when the a_{1g} band get partially populated and finally goes into the OSMP.

In Fig.5 (a)-(c), we plot the occupancy of a_{1g} band under fixed Coulomb interaction strength U as a func-

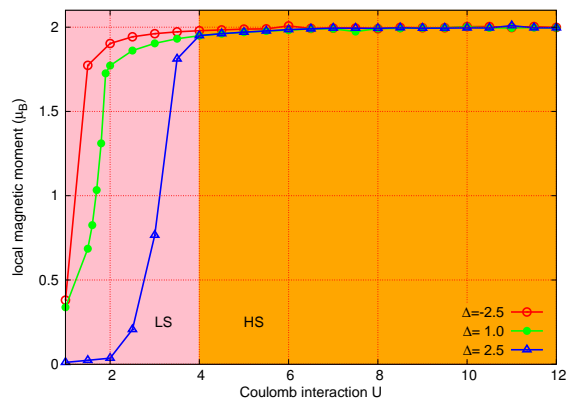


FIG. 7. (Color online) The calculated effective local magnetic moment $\sqrt{\langle S_z^2 \rangle}$ for three-band Hubbard model with rotationally invariant interaction terms. The calculations are done by DMFT+CTQMC method at finite temperature $T = 0.01$. In this figure, only the calculated results for representative crystal field splitting values ($\Delta = -2.5, 1.0, \text{ and } 2.5$) are presented. The pink region denotes LS phase, while orange region denotes HS phase.

tion of crystal field splitting Δ . For weak Coulomb interaction ($U = 1.0$), when the crystal field splitting is increased from very negative to very positive value, two plateaus can be found in the occupancy of a_{1g} band, which correspond to fully occupied and empty situations respectively. The occupation numbers decrease smoothly between the two plateaus corresponding to the metallic phase. For intermediate interaction strength with non-zero Hund's rule coupling J , there is additional plateau with occupancy being half filling, which corresponds to the OSMT phase which is completely absent when $J = 0$.

The redistribution of the electrons among the three orbitals is the key point for the OSMT in this system and can be understood by the effect of Hund's rule coupling, which favors the HS state with the (3,1) configuration. As for SU(N) $J = 0$ case, the redistribution of electrons is much more easy to be understood. As shown in Fig.6, the correlation effect induced by the Coulomb interaction increases the occupation of a_{1g} band for $\Delta < 0$ case and decreases it for $\Delta > 0$ case, which is consistent with the results obtained by Hartree-Fock mean-field method.

C. HS-LS transition

In this subsection, we focus on the magnetic properties of the three-band model during the phase transitions which have been reported rarely in the references. In Fig.7 we plot the evolution of the mean instantaneous moment, which is defined as $\sqrt{\langle S_z^2 \rangle}$, as the function of Coulomb interaction strength U with selected crystal field splitting Δ . We find that although the overall behavior looks quite similar for positive and negative crystal field splitting, the underlying physics are very different

for the two cases.

For the negative crystal field splitting $\Delta < 0$, with the increment of Coulomb interaction strength and Hund's rule coupling, the system is approaching the (2, 2) configuration (two electrons in both a_{1g} and e'_g bands). The HS state can be reached smoothly when the two electrons in the e'_g bands fall into the triplet state due to the Hund's rule coupling. At the mean while, the Mott transition happens when the spin state gets close to the HS state.

Nevertheless, the situation on the positive crystal field splitting side $\Delta > 0$ is very different. Under weak Coulomb interaction, the occupation numbers of the system are more close to the (4, 0) configuration (all the four electrons are in e'_g bands). With the increment of Coulomb interaction strength and Hund's rule coupling, when the crystal field splitting is still not strong enough to drive the system into the band insulator, the system undergoes two sequential transition. The first transition is more related to the charge transfer from the e'_g bands to a_{1g} band and the system changes from (4, 0) to (3, 1) configuration afterwards. This transition comes from the competition between the crystal field splitting, which favors the (4, 0) configuration, and the Hund's rule coupling, which favors the (3, 1) configuration. After the first transition, which manifests itself in Fig.7 as a clear kink in the $\sqrt{\langle S_z^2 \rangle} - U$ curve, the a_{1g} band is half filling and the e'_g bands are only quarter filling. Since the system with half filling is always much closer to a Mott transition, the a_{1g} band becomes Mott insulator first after the first transition, while the e'_g bands still remain metallic. A second transition happens by further increasing the Coulomb interaction together with the Hund's rule coupling, after which the system becomes Mott insulator for all the bands with the spin state being very close to a pure HS state.

IV. CONCLUDING REMARKS

We have studied the Mott transition in the three-band Hubbard model with orbital degeneracy lifting by crystal field splitting. By using the DMFT+CTQMC method and RIGA method, we have investigated how the orbital

level splitting and the Hund's rule coupling affect the Mott transition in a system with four electrons per site. We obtain the following conclusions.

Firstly, the Hund's rule coupling J (more specifically, the Ising-type Hund's rule coupling J_z) is the minimal requirement to induce OSMT and stabilize OSMP. In the phase diagram for three-band Hubbard model with rotationally invariant interactions, the OSMP covers a wide parameter range. While in the phase diagram for three-band Hubbard model without Hund's rule coupling terms, though the Mott MIT occurs when the Coulomb interaction strength reaches critical values, but the OSMP is absent.

Secondly, the interplay between crystal field splitting and Hund's rule coupling terms induces the redistribution of electrons among the three bands and leads to the complex phase diagrams. For examples, the (4,0) electronic configuration is corresponding to a band insulator phase, (3,1) configuration leads to OSMP or Mott insulator phase, and (2,2) configuration leads to metal plus band insulator or Mott insulator plus band insulator.

Thirdly, the appearance of the OSMP in this system is always accompanied by a HS-LS spin state crossover. In the OSMP, the electron distribution keeps in (3,1) configuration, which strongly favors the HS state and lowers the Hund's rule energy. When the Coulomb interaction is reduced, the OSMP collapses to metal phase accompanied by a HS-LS transition.

Finally, three-band models arise in a number of other physically important contexts, including doped C_{60} , ruthenates, etc. Extending our results to models with more realistic density of states is of high priority for future research.

ACKNOWLEDGMENTS

We acknowledge financial support from the National Science Foundation of China and that from the 973 program of China under Contract No.2007CB925000 and No.2011CBA00108. The DMFT+CTQMC calculations have been performed on the SHENTENG7000 at Supercomputing Center of Chinese Academy of Sciences (SC-CAS).

¹ M. Imada, A. Fujimori, and Y. Tokura, Rev. Mod. Phys. **70**, 1039 (1998).

² A. Georges, G. Kotliar, W. Krauth, and M. J. Rozenberg, Rev. Mod. Phys. **68**, 13 (1996).

³ Y. Tokura and N. Nagaosa, Science **288**, 462 (2000).

⁴ C.-K. Chan, P. Werner, and A. J. Millis, Phys. Rev. B **80**, 235114 (2009).

⁵ P. Werner and A. J. Millis, Phys. Rev. Lett. **99**, 126405 (2007).

⁶ V. I. Anisimov, I. A. Nekrasov, D. E. Kondakov, T. M. Rice, and M. Sigrist, Eur. Phys. J. B **25**, 191 (2002).

⁷ G. Kotliar, S. Y. Savrasov, K. Haule, V. S. Oudovenko, O. Parcollet, and C. A. Marianetti, Rev. Mod. Phys. **78**, 865 (2006).

⁸ S. Florens, A. Georges, G. Kotliar, and O. Parcollet, Phys. Rev. B **66**, 205102 (2002).

⁹ A. O. Shorikov, Z. V. Pchelkina, V. I. Anisimov, S. L. Skornyakov, and M. A. Korotin, Phys. Rev. B **82**, 195101 (2010).

¹⁰ J. Kunes, A. V. Lukoyanov, V. I. Anisimov, R. T. Scalettar, and W. E. Pickett, Nature Materials **7**, 198 (2008).

¹¹ L. Craco, M. S. Laad, and E. Müller-Hartmann, Phys.

- Rev. B **74**, 064425 (2006).
- ¹² A. Koga, N. Kawakami, T. M. Rice, and M. Sigrist, Phys. Rev. Lett. **92**, 216402 (2004).
- ¹³ A. Koga, N. Kawakami, T. M. Rice, and M. Sigrist, Phys. Rev. B **72**, 045128 (2005).
- ¹⁴ A. Liebsch, Phys. Rev. Lett. **91**, 226401 (2003).
- ¹⁵ A. Liebsch, Phys. Rev. B **70**, 165103 (2004).
- ¹⁶ C. Knecht, N. Blümer, and P. G. J. van Dongen, Phys. Rev. B **72**, 081103 (2005).
- ¹⁷ R. Arita and K. Held, Phys. Rev. B **72**, 201102 (2005).
- ¹⁸ P. G. J. v. Dongen, C. Knecht, and N. Blümer, Phys. Status Solidi (B) **243**, 116 (2006).
- ¹⁹ M. Ferrero, F. Becca, M. Fabrizio, and M. Capone, Phys. Rev. B **72**, 205126 (2005).
- ²⁰ P. Werner, E. Gull, and A. J. Millis, Phys. Rev. B **79**, 115119 (2009).
- ²¹ E. Jakobi, N. Blümer, and P. van Dongen, Phys. Rev. B **80**, 115109 (2009).
- ²² M. Neupane, P. Richard, Z.-H. Pan, Y.-M. Xu, R. Jin, D. Mandrus, X. Dai, Z. Fang, Z. Wang, and H. Ding, Phys. Rev. Lett. **103**, 097001 (2009).
- ²³ L. de' Medici, S. R. Hassan, M. Capone, and X. Dai, Phys. Rev. Lett. **102**, 126401 (2009).
- ²⁴ L. de' Medici, A. Georges, and S. Biermann, Phys. Rev. B **72**, 205124 (2005).
- ²⁵ T. Kita, T. Ohashi, and N. Kawakami, Phys. Rev. B **84**, 195130 (2011).
- ²⁶ P. Werner and A. J. Millis, Phys. Rev. B **74**, 155107 (2006).
- ²⁷ P. Werner, A. Comanac, L. de' Medici, M. Troyer, and A. J. Millis, Phys. Rev. Lett. **97**, 076405 (2006).
- ²⁸ E. Gull, A. J. Millis, A. I. Lichtenstein, A. N. Rubtsov, M. Troyer, and P. Werner, Rev. Mod. Phys. **83**, 349 (2011).
- ²⁹ E. Gull, P. Werner, S. Fuchs, B. Surer, T. Pruschke, and M. Troyer, Comput. Phys. Comm. **182**, 1078 (2011).
- ³⁰ J. Bünemann, W. Weber, and F. Gebhard, Phys. Rev. B **57**, 6896 (1998).
- ³¹ J. Bünemann, F. Gebhard, T. Ohm, S. Weiser, and W. Weber, Phys. Rev. Lett. **101**, 236404 (2008).
- ³² X. Deng, L. Wang, X. Dai, and Z. Fang, Phys. Rev. B **79**, 075114 (2009).
- ³³ N. Lanatà, H. U. R. Strand, X. Dai, and B. Hellsing, Phys. Rev. B **85**, 035133 (2012).
- ³⁴ L. de' Medici, J. Mravlje, and A. Georges, Phys. Rev. Lett. **107**, 256401 (2011).